



Changes in the diurnal temperature range over East Asia from 1901 to 2018 and its relationship with precipitation

Xiubao Sun^{1,2,3} · Chunzai Wang^{1,2,3} · Guoyu Ren^{4,5}

Received: 23 July 2020 / Accepted: 10 May 2021 / Published online: 19 June 2021

© The Author(s), under exclusive licence to Springer Nature B.V. 2021

Abstract

Since the 1950s, the East Asian diurnal temperature range (DTR), defined as the difference between the daily maximum (T_{\max}) and minimum temperatures (T_{\min}), has gradually decreased. Precipitation changes have often been cited as a primary cause of the change. However, the East Asian DTR change before 1950 and its relationship with precipitation remain unclear. Here, we used a newly developed China Meteorological Administration–Land Surface Air Temperature dataset v1.1 to examine the climatological patterns and long-term trends of the DTR in East Asia from 1901 to 2018 and its relationship with precipitation. The mean annual DTR averaged over East Asia for 1951–2018 was approximately 10.0 °C. East Asian DTR changes during 1901–2018 show two distinct characteristics. First, the DTR decreased significantly by approximately 0.60 °C during 1901–2018, and the decrease rate in the second half of the twentieth century (by ~ 0.53 °C) was significantly larger than that over the rest of the Northern Hemisphere and the global land due to rapid urbanization over East Asia. Second, before the 1950s, the DTR in East Asia showed a significant non-linear increase especially in middle latitude areas, mainly due to the warming rate of T_{\max} is higher than that of T_{\min} . Additionally, we found that the spatial pattern of long-term DTR change shows a significant negative correlation with mean precipitation patterns except in arid and semi-arid areas during 1901–2018. The decreasing trend of DTR gradually became smaller from arid regions to humid regions during 1901–2018, mainly because the difference between T_{\max} and T_{\min} warming rate gradually became smaller.

Keywords DTR · Long-term trends · Precipitation · East Asia

This article is part of the topical collection on *Historical and recent change in extreme climate over East Asia* edited by Guoyu Ren, Danny Harvey, Johnny Chan, Hisayuki Kubota, Zhongshi Zhang, and Jinbao Li.

✉ Chunzai Wang
cwang@scsio.ac.cn

Extended author information available on the last page of the article

1 Introduction

Daily maximum (T_{\max}) and minimum (T_{\min}) surface air temperatures have shown significant asymmetric warming since the 1950s over most land areas, with more significant increases in nighttime T_{\min} than in daytime T_{\max} , resulting in decreases in the diurnal temperature range (DTR; $\text{DTR} = T_{\max} - T_{\min}$) worldwide (e.g., Karl et al. 1991; Easterling et al. 1997; Vose et al. 2005; Alexander et al. 2006; Thorne et al. 2016; Sun et al. 2019). The DTR is coupled to cloudiness, precipitation, soil moisture, and evaporation; thus, its change can provide insights into changes in the hydrological cycle (Dai et al. 1997, 1999). Moreover, previous studies have also found that DTR changes significantly impact crop yields (Lobell 2007) and ecosystems (Vasseur et al. 2014). Therefore, it is important to study the characteristics and causes of DTR changes under global warming.

Previous studies have tried to determine the causes of the long-term global and regional DTR changes. It has been found that changes in the DTR are directly related to the surface solar radiation (Makowski et al. 2009; Wild 2012; Wang and Dickinson 2013). Decreases in the DTR driven by cloud cover, precipitation, and the related soil moisture after 1950 all resulted from their asymmetrical impacts on the surface solar radiation and evaporative cooling that directly affect daytime T_{\max} (Dai et al. 1997, 1999; Zhou et al. 2009). Among these factors, precipitation may affect daytime T_{\max} and thus the DTR through its association with clouds (which affect solar radiation and thus T_{\max}), its impact on soil moisture (which affects surface evaporation and thus T_{\max}), or its direct cooling effect on daytime T_{\max} (Dai et al. 1997, 1999). The negative correlation between the DTR and precipitation results mainly from precipitation's association with cloudiness and soil moisture (Dai et al. 1997; Zhou et al. 2009). This significant negative correlation between precipitation and the DTR was found to be especially apparent in the warm season (Zhou et al. 2009), as dry conditions are more associated with solar radiation and less associated with evaporative cooling (Trenberth and Shea 2005). In addition, greenhouse gases, aerosols, land-use changes (e.g., urbanization), and other climate factors can also indirectly cause DTR changes by affecting clouds and solar radiation (Gallo et al. 1996; Braganza et al. 2004; Wang et al. 2012).

As a rapidly developing region, East Asia has experienced unprecedented economic growth, resulting in great changes to the natural environment. Previous studies have found that the DTR over East Asia has decreased significantly since the 1950s (e.g., Zhai and Pan 2003; You et al. 2016; Liu et al. 2016; Sun et al. 2017a). However, the causes for the decline in the DTR over East Asia since the 1950s are not consistent with those worldwide. The decrease in the DTR in East Asia could not be explained by cloud cover (Dai et al. 1999), but is also related to the changes of aerosol increases (Liu et al. 2016), land-use changes (Ren and Zhou 2014), atmospheric water vapor (Zhao 2014), and precipitation (Shen et al. 2014). Among these factors, atmospheric water vapor and precipitation can statistically explain more than 40% of the DTR decrease over China since the 1950s (Zhao 2014; Shen et al. 2014), but physically water vapor may only have a small effect on the DTR (Dai et al. 1999). However, due to the limitation of early data quality, the previous studies on East Asian DTR mainly started in the 1950s. The change in the DTR over East Asia from 1901 to 1950 and its relationship with precipitation have not yet been investigated. In this study, we use the China Meteorological Administration–Land Surface Air Temperature dataset v1.1 (CMA-LSAT v1.1) to analyze the climatology and long-term characteristics of DTR changes over East Asia for the period from 1901 to 2018 and then examine the association of T_{\max} , T_{\min} , and DTR changes on precipitation in East Asia.

The rest of the paper is organized as follows. The data and methods used in this study are introduced in Sect. 2. In Sect. 3.1, we analyze the climatological characteristics of the DTR over East Asia from 1951 to 2018. Then, the DTR trend and its dependence on precipitation over East Asia are presented in Sects. 3.2–3.3. There are some discussions in Sect. 4. Finally, a summary of the key findings is given in Sect. 5.

2 Data and methods

2.1 Data

2.1.1 Temperature data

In the present study, the DTR is defined as the difference between the daily T_{\max} and T_{\min} . The observational T_{\max} and T_{\min} data are from the CMA-LSAT v1.1 dataset (see [supplementary material](#) for the detailed dataset introduction), which provides homogenized temperatures from 1901 to 2018 over global land derived from observations made at weather stations (Sun et al. 2017b; Xu et al. 2017). CMA-LSAT v1.1 data cover East Asia (80°–150°E, 0°–60°N) fairly uniformly, especially in the northwest of East Asia (Sun et al. 2017b; Xu et al. 2017). For example, 24 stations in China, which have more than 100 years of records, are added to the new dataset.

In this study, to reduce the uncertainty of DTR calculation results throughout the whole research period and ensure that all East Asian stations have long enough observation records in the base period 1961–1990, we select stations according to the following selection standards:

Case 1: To ensure that the observation records of stations in the climate reference period are relatively complete, we only select stations with records of at least 15 years in the base period and at least 3 years of records for every 10 years during the base period 1961–1990.

Case 2: If there are 2 months of missing values in a year, the year will be recorded as missing values.

Case 3: Because there are noticeable differences between the DTR on land and islands, we only choose the observation stations on land and remove the island stations in the western Pacific, the Indian Ocean, and the South China Sea far away from the mainland.

Case 4: According to the principle of retaining as many stations as possible, only stations with records longer than 30 years are selected when constructing the time series during 1901–2018. Meanwhile, cases 1 and 2 should also be met.

Case 5: In the process of calculating the series and grid box trends in the periods 1901–1950 and 1951–2018 (Sect. 3.2), in order to reduce the impact of short record stations, only stations with more than 25 years of observation records in the periods 1901–1950 and 1951–2018 are selected to participate in the calculation.

Case 6: In the process of determining the difference in the time series of stations with different record lengths (Sect. 3.2), we also select stations with more than 100 years of records to participate in the comparison.

Finally, according to cases 1–4, we select 1968 stations in East Asia that met these conditions over East Asia (Table 1). To reduce the uncertainty caused by the stations' non-uniform spatial

distribution, we divided all the stations into 124 grid boxes with a resolution of $5^\circ \times 5^\circ$. Figure 1a–c shows the spatial distribution of stations in the periods 1901–1920 (a), 1920–1940 (b), and 1940–1960 (c) over East Asia. Before 1920, East Asia stations (total 178) are mainly distributed in Japan, Russia, Philippines, India, southeast China, and northeast China (Fig. 1a). From 1920 to 1940, the number of stations increased to 695 (Fig. 1b). From 1940 to 1960, the number of stations increased rapidly to 1666 (Fig. 1c), and the number of stations is close to that of all stations from 1901 to 2018 (Fig. 1d). Figure 1e shows that stations and grid boxes' coverage increased rapidly from 1920 to 1950, reaching 50% in 1933 and stabilizing at more than 80% after 1950.

Considering the differences in the DTR between the marine continental region and inland, we divided East Asia into three 20° latitude zones for sub-regional study. Before the 1940s, the grid box coverage in mid-latitudes is significantly higher than in low-latitudes. The grid box coverage of low latitudes, mid-latitudes, and high latitudes reached 50% in 1950, 1925, and 1933, respectively (Fig. 1f).

Consequently, East Asian stations before 1920 are mainly distributed in Japan, Russia, Philippines, India, southeast China, and northeast of China. From then on, the coverage of stations and grid boxes increased rapidly, reaching 50% in 1933 and stabilizing at more than 80% after 1950. Therefore, it can be considered that the DTR changes after 1933 have relatively higher credibility.

In addition, it is worth mentioning that both East Asia and low- and mid-latitude regions have experienced a decline in grid box coverage and stations in the 1930s–1940s. To explore whether the reduction in grid box coverage dominates the low DTR values in the 1930s, we will clarify this problem by comparing different time series in Sect. 3.2.

2.1.2 Other data

To analyze the association of the DTR with precipitation, rain gauge precipitation data from the China Meteorological Administration-Global Historic Precipitation dataset (Yang et al. 2016) are also used. We only selected stations with at least 15 years (30 years) of observational records in the base period 1961–1990 (during 1901–2018). We only use the precipitation grid boxes to match the DTR grid boxes (see Supplementary material Fig. S1). The number of match grid boxes is also close to the number of all DTR grids. This suggests that the precipitation data is relatively reliable.

In addition, to further assess the uncertainty caused by urbanization, 2010 land cover data from satellite remote sensing with a resolution of 300 m from the European Space Agency (Hollmann et al. 2013) is used in this study to distinguish between urban and rural stations.

Table 1 Station information in East Asia and three different latitude zones. Grid box coverage (%) defined as the number of grid boxes in the certain year divided by the maximum number of grid boxes in a year during 1901–2018

Region	Stations with a record length of 118 years	Number of stations in 1920	Number of stations in 1940	Total stations	Grid box coverage >50% year/stations
Low latitude (0–20°N)	5	26	58	193	1950/78
Middle latitude (20–40°N)	55	96	404	1134	1925/136
High latitude (40–60°N)	10	56	233	641	1933/93
East Asia	70	178	695	1968	1933/270

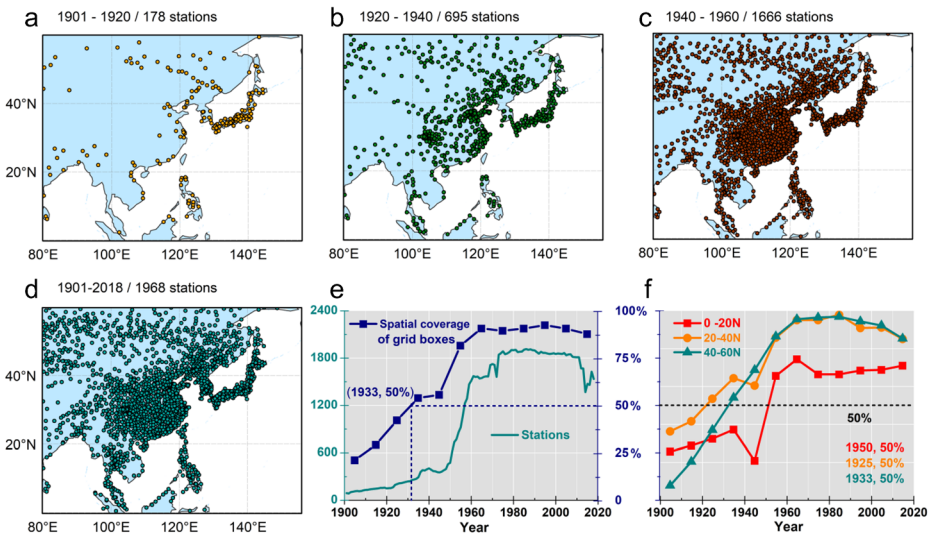


Fig. 1 (a–d) Spatial distribution of stations in different periods over East Asia land (80°–150°E; 0°–60°N) and (e, f) the long-term change of stations and grid box coverage during 1901–2018. Grid box coverage (%) in (e, f) is defined as the number of grid boxes in the certain year divided by the maximum number of grid boxes in a year during 1901–2018. The dark blue curve and the green curve in (e) represent all the stations and grid box coverage in East Asia, respectively. Different color curves in (f) represent grid box coverage changes in different latitudes. The combination of years and numbers in (e) and (f) represents the year when the grid box coverage began to exceed 50%

The NCAR/NCEP twentieth-century reanalysis version 2 (interpolated to 5° resolution grid boxes) is used to estimate the grid box coverage error. The CRUTS4.0.3 grid data from 1901 to 2018 are used to compare with the CMA-LSAT v1.1 data. Before comparison, the data is interpolated to 5° resolution grid boxes.

2.2 Methods

2.2.1 Grid box coverage error and urbanization impact estimation method

There are some uncertainties in the long-term changes of land surface air temperature, especially before the 1950s (Jones 1994; Brohan et al. 2006). Even if the stations are selected strictly according to Sect. 2.1.1, there are still some uncertainties throughout the study period. The primary sources of uncertainty in the current estimation of land temperature series are station error, grid box coverage error, urbanization, etc. (Brohan et al. 2006; Li et al. 2010; Du et al. 2012).

Referring to the method used by Du et al. (2012), the grid box coverage error is estimated approximately based on the NCAR/NCEP twentieth century reanalysis data. Taking a grid box as an example, the estimation method is as follows: First, according to the observation grid boxes, obtain sampling grid boxes from complete reanalysis grid boxes by sampling; Second, we can obtain complete time series and sampling time series on the grid box scale, then the difference between two series is the difference series on grid box scale; Finally, for East Asia as a whole, we calculate the standard deviation of the difference series across all grid boxes in East Asia for a certain year, which is the grid box coverage error for the certain year.

We use the isolated forest algorithm in the machine learning method invented by Zhang et al. (2021) to select urban and rural stations. Calculation steps: first, we set the United States Climate reference network (USCRN) as a standard climate network, and then use the land use data around USCRN from the European Space Agency to train the model parameters; Second, the trained parameters in the first step are substituted into the isolated forest model, and then the Asian stations in 2010 are classified into urban stations and rural stations through the model (see [supplementary material](#) for detailed method introduction). Finally, East Asian stations in 2010 can be divided into 1436 urban stations and 346 rural stations (see [Supplementary material Fig. S2a,b](#)). The urbanization land within 12 km around the rural station is less than 5%.

The main purpose of using land use data in 2010 is to ensure that stations defined as rural are not affected by urbanization until the last few years. At the same time, using the 2010 land use data can avoid missing some stations due to data updates in the past five years. However, it may still include some problems such as the relocation of stations, and the residual urbanization effect in the rural data series due to the lack of real rural stations. As a result, the impact of urbanization will be underestimated to a certain extent. Therefore, the conclusion of the urbanization impact estimation by this method is a conservative estimate and will not overestimate the urbanization impact.

The formula for the urbanization contribution rate (C_u) is as follows (Ren and Zhou 2014):

$$C_u = |\Delta T_{\text{all-rural}}/T_{\text{all}}| \times 100\%$$

where $\Delta T_{\text{all-rural}} = T_{\text{all}} - T_{\text{rural}}$, T_{all} and T_{rural} represent the temperature series of all stations and rural stations.

2.2.2 Other methods

Classification of dry/wet regions: According to annual mean precipitation in every grid box, we divided East Asia into four different dry and wet regions. An annual mean precipitation of 0–400 mm, 400–800 mm, 800–1600 mm, and more than 1600 mm are used to indicate arid and semiarid areas, semi-humid areas, humid areas, and extremely humid areas, respectively. The precipitation grid boxes used in calculation are those matching DTR.

We first averaged the station T_{min} , T_{max} , and DTR anomalies (relative to 1961–1990) within each grid box to derive the grid box mean value, requiring at least one station with data within each box. The gridded anomaly data were regionally averaged over East Asia (overland boxes only) with the grid box area as weight. The linear trends of the anomaly series were obtained by using the least-squares fitting, and the significance of the linear trends is judged using the two-tailed Student's *t* test. The trend is considered statistically significant if it is significant at the 5% ($p < 0.05$) significance level.

3 Results

3.1 Climatological characteristics of the DTR over East Asia

In this section, we use all available observation records to calculate the climatological characteristics of the DTR in East Asia and three sub-regions during 1951–2018, as shown in [Fig. 2a,b](#). The observed annual mean DTR over East Asia is approximately 10.0 °C (2.8–

18.8 °C). From the spatial patterns (Fig. 2a), we can determine that the DTR gradually increased from coastal to the Asian continent, and the DTR of the marine continent (0–20 °N) and coastal grid boxes are significantly lower than those of inland grid boxes. Larger DTR is seen in northwest China and the Hindu Kush–Himalayas region, where the annual mean DTR is more than 12.5 °C. On the other hand, with the increase of latitude, the proportion of land stations increases, and the zonal average DTR increases (Fig. 2b). In addition, the DTR in the northwest of East Asia is smaller than that in the surrounding area, which indicates that the DTR does not increase with latitude, and the DTR in the zonal average shows the difference in the distribution of sea and coastal grid boxes. Furthermore, the annual cycle of the DTR over East Asia is smaller in the warm season than in the cold season, and the amplitude at high latitudes is larger than that at low latitudes (Fig. 2b).

3.2 Long-term changes in the DTR over East Asia

Fig. 3a shows the long-term time series for the DTR (dark blue curve) over East Asia during 1901–2018 based on CMA-LSAT v1.1 data. The DTR change in East Asia shows a significant long-term decrease. The DTR decreased by 0.60 °C during 1901–2018. The dominant characteristics of the DTR in East Asia before and after the 1950 are different. From 1951 to 2018, the DTR of East Asia showed a significant decrease of 0.53 °C. Before 1950, the DTR shows non-linear increasing. The reason for the non-linear change is mainly due to the low value of DTR in the 1930s. Additionally, we compare the time series of different data sources to verify the credibility of the long-term changes in DTR. Furthermore, the primary purpose of comparing time series with different record lengths is to verify whether the change in DTR is caused by the increase of stations.

Figure 3a shows the comparison of the CMA-LSAT series and CRUTS4 series. In general, both the CMA-LSAT time series and the CRUTS4 time series show the uniform characteristics of a slow increase trend in the first half of the twentieth century and a significant decrease in the second half of the twentieth century, and both of them also have a low DTR value in the 1930s. The high value of DTR in 1940s–1950s is more evident in the CMA-LSAT series than

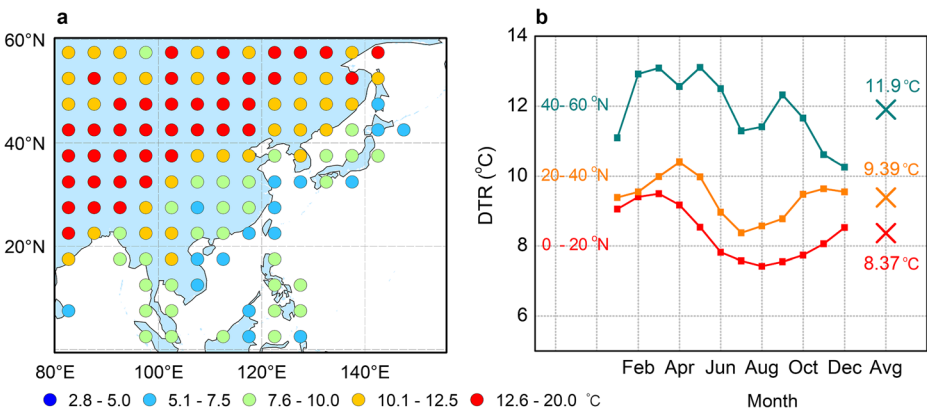


Fig. 2 (a) Climatological distribution of annual mean DTR from 1951 to 2018 based on the CMA-LAST v1.1 dataset, and (b) annual cycle of mean DTR in different latitudes. The Xs with different colors in (b) represent the annual mean DTR in different latitudes

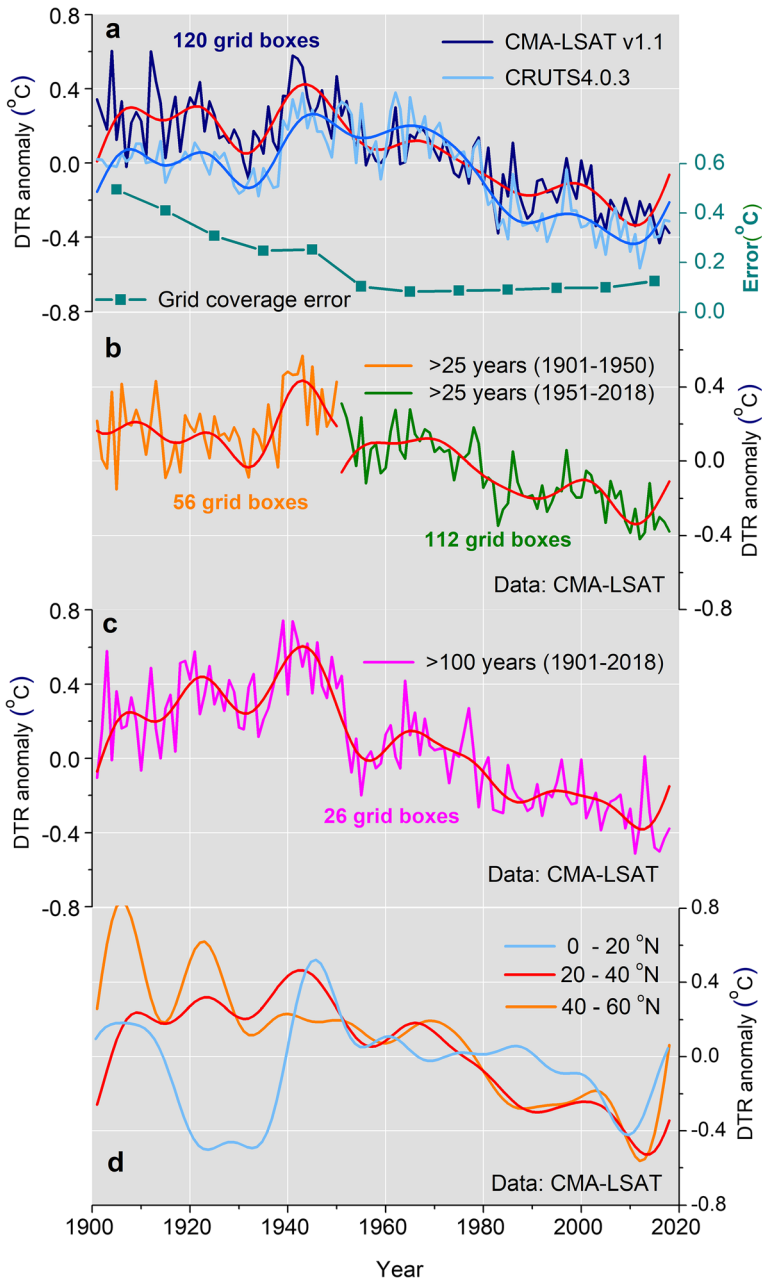


Fig. 3 (a) Long-term time series for the DTR over East Asia during 1901–2018 based on CMA-LSAT v1.1 (dark blue curve), and CRUTS4.0.3 (blue curve); the green curve represents the grid box coverage error in CMA-LSAT series. (b) East Asian DTR time series in the two periods of 1901–1950 and 1951–2018, only selected stations with records for more than 25 years in the above two periods. (c) East Asian DTR time series based on more than 100 years of observational records. (d) The 11-year smooth curve of the DTR in different latitude zones. All the smooth curves in the figure are 11 years smooth. All the anomalies are relative to the base period 1961–1990

in the CRUTS4 series. Before the 1950s and after the 1980s, the CRUTS4 series is obviously lower than the CMA-LSAT series.

It is worth noting that the East Asian grid box coverage only reached 50% in 1933, and then increased to more than 80% after 1950, which implies that the results of DTR estimation before the 1950s, especially before the 1930s, may contain great uncertainty. Therefore, we estimate the grid box coverage error of East Asian DTR for each decade, and the results are shown in Fig. 3a (green line). It can be found that the uncertainty of the DTR remained at very high levels before the 1950s (more than 0.2 °C), and then the uncertainty level decreases with the increasing of grid boxes. After the 1950s, the grid box coverage error decreased to approximately 0.1 °C.

Figure 3b,c shows a piecewise time series based on stations with a record length longer than 25 years before and after 1950 (Fig. 3b), and a long record series based on stations with a record length of more than 100 years (Fig. 3c). Overall, the two time series and all station series (Fig. 3a dark blue curve) have relatively consistent interdecadal fluctuations before the 1940s. The difference is that the DTR of the long record series is lower before 1920s and higher in the 1950s than the all station series, which results in an increase trend of DTR before the 1950s. In addition, all station time series, long record time series, and piecewise time series show low DTR values in the 1930s. This suggests that the reduction in grid box coverage during the 1930s to 1940s does not cause the low DTR values.

Figure 3d compares the 11 years smooth of the DTR series in three latitudes during 1901–2018. The DTR of the three sub-regions decreased significantly after the 1950s. Before the 1950s, the DTR in high and middle latitudes show decrease and increase, respectively. Because there are few stations in the low latitude marine continental region before 1950, the DTR in low latitude changes always with a wide range of changes. Although the low-latitude DTR fluctuates greatly, the grid is less before 1950, and therefore it cannot have too much influence on the average large-scale DTR in East Asia. The DTR trend reversal phenomenon occurs only in the mid-latitude of 20–40 °N. This trend reversal phenomenon is similar to that reported for the global DTR by Sun et al. (2019).

With regard to DTR spatial distribution in different periods, there are also obvious differences in DTR changes. To minimize the impact of short-time series stations on the trend estimation of DTR, we only select stations with records longer than 25 years in the periods 1901–1950 and 1951–2018. After 1950, the DTR over East Asia shows a decreasing trend at widespread locations, especially at broad land stations. Before 1950, the grid boxes constructed by stations with a record length of more than 25 years are mainly distributed in East China, Russia, Japan, and the Philippines. Before 1950, the low latitude shows a significant decreasing trend. In the middle latitudes, 86% of the grids show a significant increase in DTR. The grid boxes with a significantly decreased and increased trend in high latitude account for 50% and 50%, respectively.

Furthermore, we also evaluated the effect of T_{\max} and T_{\min} on DTR changes in these two periods. Figure 4b shows the relationship between T_{\max} and T_{\min} trends and DTR trends in 1901–1950 and 1951–2018. The warming rate of T_{\min} has been more extensive than that of T_{\max} in the periods 1901–1950 and 1951–2018, which directly caused the significant decline in the DTR. The DTR's dependence on T_{\max} shows differences in different periods (Fig. 4c,d red lines). Before 1950, the DTR increases significantly with the increase in T_{\max} , but after 1951, the DTR's dependence on the increase in T_{\max} weakened. These conclusions indicate that nonuniform changes of T_{\max} dominate the difference of DTR trend in different periods. Simultaneously, the long-term rapid increase in T_{\min} caused the decline in the DTR.

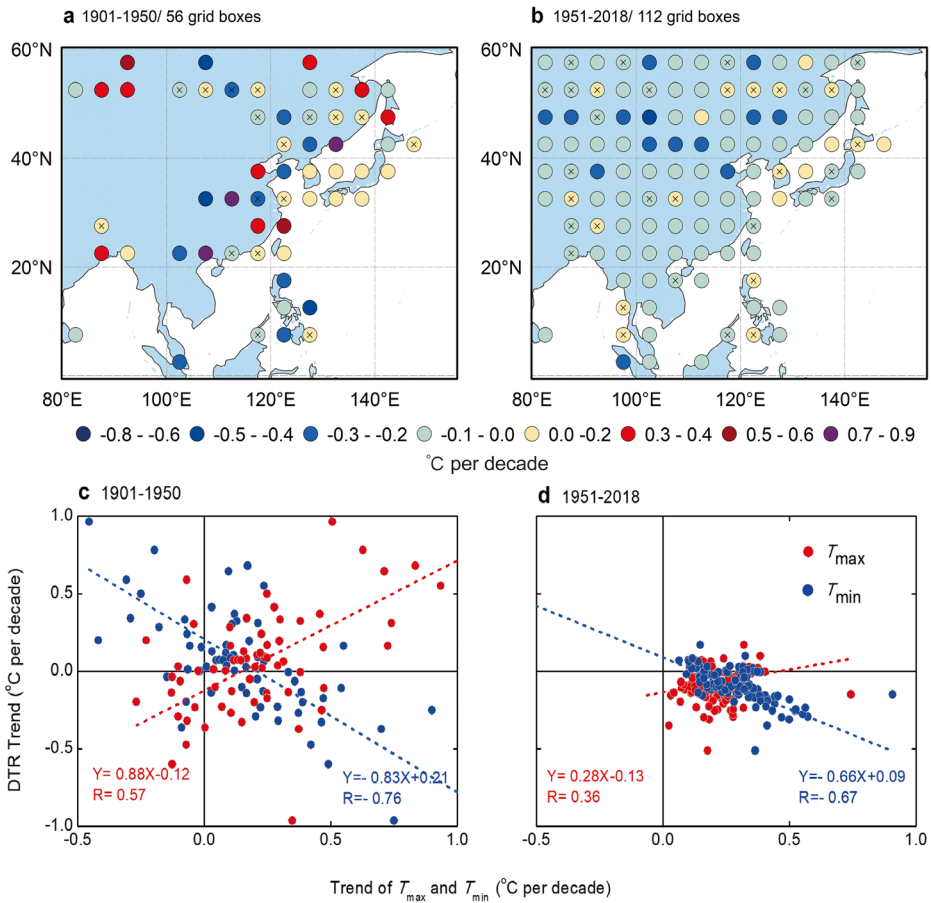


Fig. 4 (a, b) Spatial distribution of the East Asian DTR trend in 1901–1950 and 1951–2018. The grid boxes marked with X represent the trend is not statistically significant ($p > 0.05$). (c, d) The relationship between T_{max} (red), T_{min} (blue) trends, and the DTR trends in 1901–1950 and 1951–2018. The red and blue dot lines represent the linear trends of the relationship between T_{max} , T_{min} , and the DTR, respectively

To determine whether the DTR change is seasonal, we also calculate DTR trends over the whole study period (Fig. 5). In general, the long-term decrease of the DTR exists in all seasons, but the magnitude of the changes is different. The decreasing trend in winter (DJF) is often larger than that in the other three seasons. These conclusions are also consistent with the characteristics of DTR changes over East Asia since 1950 reported by Liu et al. (2016, 2018).

3.3 Relationship between the DTR and precipitation over East Asia

Although precipitation has no direct effect on DTR, it could indirectly affect DTR by affecting cloud cover and solar radiation, etc. To determine the indirect role of precipitation in changes of the DTR over East Asia, we examined the association between DTR and precipitation. In general, there is a significant negative correlation between the DTR and precipitation over East Asia during 1901–2018. Furthermore, we also found that the association between the DTR and precipitation is not significant in arid and semiarid regions, but correlations are significantly

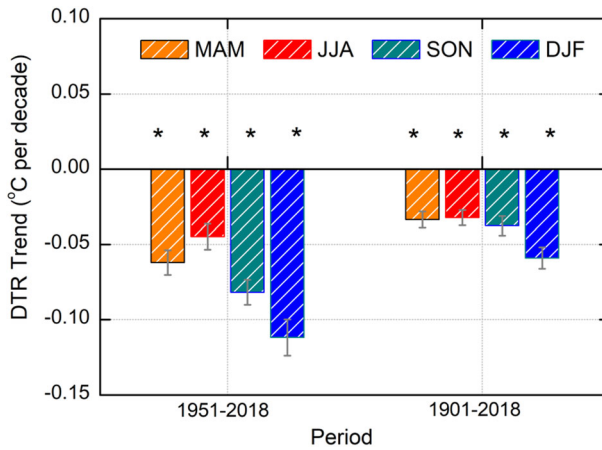


Fig. 5 Seasonal trends of the DTR in different periods. The orange, red, green, and blue bars represent the DTR trends for spring (MAM), summer (JJA), autumn (SON), and winter (DJF) in the Northern Hemisphere, respectively. Statistically significant ($p < 0.05$) trends are marked with asterisks. The error bar represents twice the standard deviation

correlated in other regions (Fig. 6b). This is also similar to the conclusion that the correlation between global precipitation and the DTR in arid areas is not significant after 1950 (Zhou et al. 2009). Dai et al. (1999) indicated that the DTR in arid areas was more affected by solar radiation than by evaporative cooling. This can theoretically explain why the long-term changes in the DTR over East Asia had no significant relationship with precipitation since 1901.

To further determine the relationship between T_{max} , T_{min} , and DTR’s long-term changes to annual mean precipitation over East Asia (Fig. 6b), it is noted that from arid regions to humid regions, T_{max} and T_{min} trends show an increasing trend, but the warming rate of T_{max} relative to T_{min} is more significant from 1901 to 2018. However, the difference between T_{max} and T_{min}

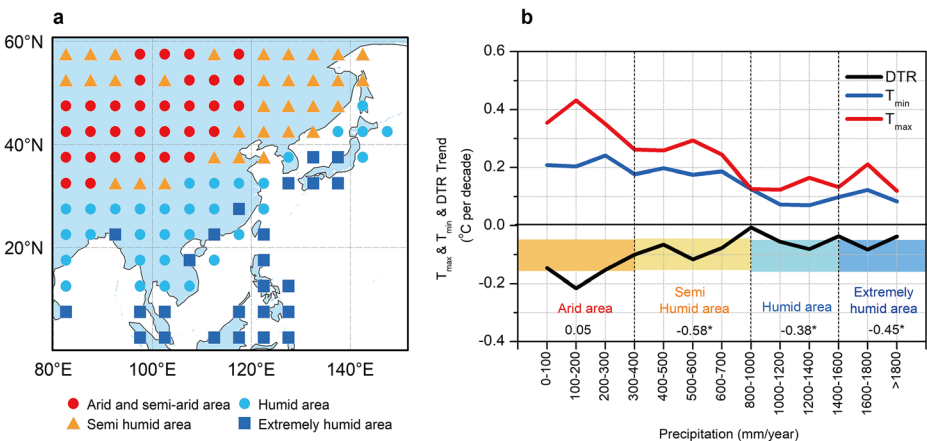


Fig. 6 (a) Different dry/wet regions and (b) average T_{max} , T_{min} , and DTR trend in different annual mean precipitation areas. The numbers in (b) represent the correlation between DTR and precipitation in different dry/wet regions during 1901–2018. Statistically significant ($p < 0.05$) trends are marked with asterisks

warming rate is gradually smaller, from arid regions to humid regions. The above causes a slower decline in DTR, from arid regions to humid regions. Although there is no direct connection between precipitation and DTR in physical processes, precipitation and DTR changes are statistically related from 1901 to 2018. The above shows that even if the direct influence factor data of DTR is lacking, the indirect factor of precipitation can also reflect the possible change characteristics of DTR.

4 Discussion

4.1 Long term decline of DTR in East Asia

Due to data limitations, previous studies mainly started from the 1950s, and few studies focused on the change of the DTR since 1901. Recent studies indicated that the rapid increase in T_{\min} in the Northern Hemisphere and the globe caused the DTR decrease since 1901 (Thorne et al. 2016; Sun et al. 2019). Table 2 shows a comparison of the global, Northern Hemisphere, and East Asian DTR changes in different studies. Since 1901, the decline of the DTR in East Asia ($-0.6\text{ }^{\circ}\text{C}$) is significantly lower than that in globe ($-0.41\text{ }^{\circ}\text{C}$) and the Northern Hemisphere ($-0.42\text{ }^{\circ}\text{C}$). After 1951, the DTR also declined rapidly in East Asia.

A previous study indicated that global temperature trends could be estimated using only 172 “independent stations” (Jones 1994). Still, the conclusion was drawn based on a basic understanding of global climate change characters. Although there is significant uncertainty in the surface temperature series before 1950, it does not mean that the temperature in that period cannot reflect the primary climate change because the temperature change can reflect the climate of a broad range (Tang et al. 2009). In the statistical, better spatial coverage can reduce uncertainty in time series (Thorne et al. 2005; Brohan et al. 2006).

The reason for the decreased global and regional DTR is generally considered to be the synergistic effects of solar radiation, cloud cover, aerosols, precipitation, water vapor, and land use (Dai et al. 1999). It is also found that the solar radiation reaching the ground shows a significant negative correlation with cloud cover and aerosol at a global or regional scale (Dai et al. 1997; Liu et al. 2016). Dai et al. (1997, 1999) found that the increase of cloud cover after 1950 could explain the global DTR’s spatial distribution by over 80%. However, cloud cover in China and East Asia cannot explain the DTR decline after 1950 (Shen et al. 2014; Liu et al. 2016). In East Asia, there were few clouds and aerosol observation stations in the first half of the twentieth century, and therefore it is not easy to evaluate these

Table 2 Comparison of changes in the DTR of East Asia, Northern Hemisphere, and global for different studies

Research	Study area	Study period	The magnitude of DTR decline ($^{\circ}\text{C}$)	
			1951–2014	1901–2014
Sun et al. (2019)	Globe	1901–2014	-0.35	-0.41
	Northern Hemisphere		-0.42	-0.42
This study	East Asia	1901–2018	1951–2018	1901–2018
			-0.53	-0.60

factors' impact on the DTR. This paper found that the DTR in East Asia has a significant correlation with precipitation during 1901–2018. Although there is no direct connection between precipitation and DTR in physical processes, precipitation and DTR changes are statistically related from 1901 to 2018. This implies that that even if the direct influence factor data of DTR is lacking, the indirect factor of precipitation can also reflect the possible change characteristics of DTR.

4.2 The impact of urbanization on DTR during 1951–2018

Urbanization is a crucial source of uncertainty in temperature trend estimation. Due to the influence of human activities, it is found that the cloud cover and aerosol level showed a significant increase in the past decades (Croke et al. 1999; Wang et al. 2009), especially in urban areas (Romanov 1999). The impact of urbanization on the DTR can generally be attributed to two interrelated mechanisms (Arnfield 2003; Oke et al. 2017; Varquez and Kanda 2018). In the daytime, the albedo of the underlying urban surface is lower than that of rural areas, and the sensible heat of the city is greater than that of the countryside due to more solar radiation being absorbed in the city. At the same time, the cooling effect of evapotranspiration in urban areas is smaller than in rural areas (Varquez and Kanda 2018). These caused the city's temperature to be much higher than that in the countryside. On the other hand, due to the city's complex three-dimensional structure, urban buildings absorb and reflect infrared radiation at night time. In addition, urban thermal inertia causes the heat absorbed in the city during the daytime and released at nighttime. The synergistic effect of the two causes leads to a more substantial heat island effect at nighttime than during daytime. The intensity of the above two causes is related to the city size (Arnfield 2003; Oke et al. 2017). Under the influence of more substantial nighttime urban heat island at night, T_{\min} in urban areas decreases more slowly than in rural areas (Ren and Zhou 2014; Jiang et al. 2020). As a result, the DTR of urban stations is usually smaller than surrounding rural stations (Yang et al. 2013; Ren and Zhou 2014; Wang et al. 2018).

East Asia is one of the regions most clearly affected by urbanization globally during the past decades (Jones et al. 2008; Ren and Zhou 2014). For example, the impact of urbanization on the annual mean temperature in China can reach 27% (Zhang et al. 2010), which is higher than the 10% global average assessed by Jones et al. (1990) and the IPCC (2013). However, stations with early observation records are mainly concentrated in large cities; thus, it is difficult to assess the impact of urbanization on the DTR before 1950 due to the lack of data from rural stations. Therefore, we only calculated the contribution rate of urbanization to T_{\max} , T_{\min} , and the DTR after 1951, applying the method by Zhang et al. (2021). The results show that the impact of urbanization on T_{\max} (25.9%) is smaller than that on T_{\min} (28.2%). This is also consistent with the conclusion that urbanization has a more noticeable impact on the nighttime temperature or T_{\min} . The impact of urbanization on the DTR reaches 43.6%, which indicates that the DTR is more sensitive to urbanization (Fig. 7). These limitations need to be addressed through early data rescue and reasonable correction for urbanization bias in future studies. Therefore, these indicate that the contribution of urbanization leads to underestimating the DTR trend. However, it cannot affect the decreasing trend of the DTR in the second half of the twentieth century. This also suggests that the DTR over East Asia decreased faster than that of the globe and the Northern Hemisphere in the second half of the twentieth century (Table 2), which is mainly due to the larger scale and more rapid urbanization in East Asia than in other regions of the global.

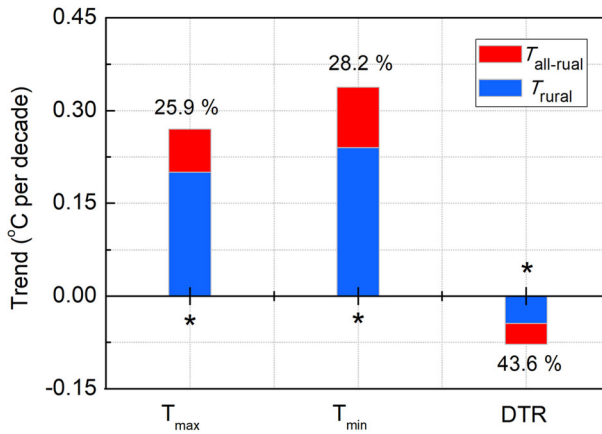


Fig. 7 The effect of urbanization on the T_{max} , T_{min} , and DTR trends over East Asia during 1951–2018. The numbers above the bars represent the contribution rates of urbanization (C_u , the calculation method of C_u is shown in Sect. 2) to different climatic factors. The blue bars represent the rural trends, and the red bars represent the impact of urbanization. The stations here only include urban stations and rural stations in 2010. Statistically significant ($p < 0.05$) trends are marked with asterisks. The unit of the trend is $^{\circ}\text{C}$ per decade

5 Summary

We selected the observation data of 1668 stations over East Asia during 1901–2018 from the CMA-LAST v1.1 dataset to analyze the climatological and long-term change characteristics of the DTR over East Asia. Furthermore, we also analyzed the association between the DTR change and precipitation. The main conclusions are as follows:

- (1) The observed annual mean DTR over East Asia is approximately 10.0°C , which increases gradually from coastal to continental Asia. The DTR of the marine continent ($0\text{--}20^{\circ}\text{N}$) and coastal grid boxes are significantly lower than those of inland grid boxes.
- (2) The DTR changes over East Asia during 1901–2018 show two dominant characteristics. The first is a significant long-term decrease in the DTR, with a 0.60°C decrease from 1901 to 2018. The second is noticeable interdecadal fluctuations in the DTR before the 1940s over East Asia. Before 1950, the high latitudes and mid-latitudes, where the grid boxes coverage rate is relatively high, show nonuniform decreased and increased trend. These two dominant characteristics of the East Asian DTR are consistent with the global changes since 1901 and accompanied by prominent regional characteristics. However, compared to the globe, Northern Hemisphere, and East Asia, the decline of the DTR in East Asia (-0.6°C) is significantly lower than that in the globe (-0.41°C) and the Northern Hemisphere (-0.42°C).
- (3) This study found that the long-term spatial patterns of DTR change show a significant negative correlation with mean precipitation patterns except in arid and semi-arid areas during 1901–2018. In addition, the decreasing DTR trend is gradually smaller from arid regions to humid regions during 1901–2018, mainly because the difference between T_{max} and T_{min} warming rate is gradually smaller.
- (4) Additionally, it should be noted that the DTR is highly sensitive to urbanization, and the impacts of urbanization contribution on the current trend estimation of T_{max} , T_{min} , and DTR in East Asia reached 25.9%, 28.2%, 43.6% from 1951 to 2018, respectively. This

indicates that the DTR of East Asia decreased faster than that of the Northern Hemisphere and globe in the second half of the twentieth century, mainly due to the larger scale and more rapid urbanization in East Asia than in other regions of the globe.

Supplementary Information The online version contains supplementary material available at <https://doi.org/10.1007/s10584-021-03120-1>.

Acknowledgments We thank Panfeng Zhang for his help in classifying urban and rural stations. We thank four anonymous reviewers for their valuable comments and suggestions.

Funding This study is supported by the National Key Research and Development Program of China (2019YFA0606701 and 2018YFA0605603), the Natural Science Foundation of China (42005036 and 41731173), the Strategic Priority Research Program of Chinese Academy of Sciences (XDB42000000 and XDA20060502), the Key Special Project for Introduced Talents Team of Southern Marine Science and Engineering Guangdong Laboratory (Guangzhou) (GML2019ZD0306), Innovation Academy of South China Sea Ecology and Environmental Engineering, Chinese Academy of Sciences (ISEE2018PY06), and the Leading Talents of Guangdong Province Program.

Data availability The global land use/land cover data could be available from the ESA (www.esa-cci.org). Due to data management policy, need to contact the National Meteorological Information Center of China Meteorological Administration (<http://data.cma.cn/en>) for the access of temperature and precipitation data.

References

- Alexander LV, Zhang XB, Peterson TC et al (2006) Global observed changes in daily climate extremes of temperature and precipitation. *J Geophys Res Atmos* 111:D05109. <https://doi.org/10.1029/2005JD006290>
- Arnfield AJ (2003) Two decades of urban climate research: a review of turbulence, exchanges of energy and water, and the urban heat island. *Int J Climatol* 23:1–26 <https://doi.org/10.1002/joc.859>
- Braganza K, Karoly DJ, Arblaster JM (2004) Diurnal temperature range as an index of global climate change during the twentieth century. *Geophys Res Lett* 31:L13217
- Brohan P, Kennedy JJ, Harris I et al (2006) Uncertainty estimates in regional and global observed temperature changes: a new data set from 1850. *J Geophys Res Atmos* 111(D12). <https://doi.org/10.1029/2005JD006548>
- Croke MS, Cess RD, Hameed S (1999) Regional cloud cover change associated with global climate change: case studies for three regions of the United States. *J Clim* 12(7):2128–2134
- Dai AG, Del Genio AD, Fung IY (1997) Clouds, precipitation and temperature range. *Nature* 386(6626):665–666
- Dai AG, Trenberth KE, Karl TR (1999) Effects of clouds, soil moisture, precipitation, and water vapor on diurnal temperature range. *J Clim* 12:2451–2473
- Du YG, Tang GL, Wang Y (2012) Uncertainty for change of mean surface air temperature in China in last 100year. *Plateau Meteorol* 31(2):456–462 (in Chinese)
- Easterling DR, Horton B, Jones PD et al (1997) Maximum and minimum temperature trends for the globe. *Science* 277(5324):364–367
- Gallo KP, Easterling DR et al (1996) The influence of land use/land cover on climatological values of the diurnal temperature range. *J Clim* 9(11):2941–2944
- Hollmann R, Hollmann R, Merchant CJ, Saunders R et al (2013) The ESA climate change initiative: satellite data records 726 for essential climate variables. *Bull Am Meteorol Soc* 94:1541–1552
- IPCC (2013) Climate change 2013: the physical science basis. In: Stocker TF, Qin D, Plattner GK (eds) Contribution of working group I to the fifth assessment report of the intergovernmental panel on climate change. Cambridge University Press, Cambridge, p 1535. <https://doi.org/10.1017/CBO9781107415324>
- Jiang SJ, Wang KC, Mao YN (2020) Rapid local urbanization around most meteorological stations explain the observed daily asymmetric warming rates across China from 1985 to 2017. *J Clim* 33(20):9045–9061
- Jones PD (1994) Hemispheric surface air temperature variations: a reanalysis and an update to 1993. *J Clim* 7: 1794–1802
- Jones PD, Groisman PY, Coughlan M et al (1990) Assessment of urbanization effects in time series of surface air temperature over land. *Nature* 347(6289):169–172

- Jones PD, Lister DH, Li QX (2008) Urbanization effects in large-scale temperature records, with an emphasis on China. *J Geophys Res Atmos* 113(D16). <https://doi.org/10.1029/2008JD009916>
- Karl TR, Kukla G, Razuvayev VN et al (1991) Global warming evidence for asymmetric diurnal temperature change. *Geophys Res Lett* 18(12):2253–2256
- Li QX, Dong WJ, Li W et al (2010) Assessment of the uncertainties in temperature change in China during the last century. *Chin Sci Bull* 55(19):1974–1982
- Liu L, Li Z, Yang X et al (2016) The long-term trend in the diurnal temperature range over Asia and its natural and anthropogenic causes. *J Geophys Res Atmos* 121(7):3519–3533
- Lobell DB (2007) Changes in diurnal temperature range and national cereal yields. *Agri Forest Meteorol* 145(3–4):229–238
- Makowski K, Jaeger EB, Chiacchio M et al (2009) On the relationship between diurnal temperature range and surface solar radiation in Europe. *J Geophys Res* 114:D00D07. <https://doi.org/10.1029/2008JD011104>
- Oke TR, Mills G, Christen A et al (2017) *Urban Climates*. Cambridge University Press, Cambridge
- Ren GY, Zhou YQ (2014) Urbanization effect on trends of extreme temperature indices of national stations over mainland China, 1961–2008. *J Clim* 27(6):2340–2360
- Romanov P (1999) Urban influence on cloud cover estimated from satellite data. *Atmos Environ* 33(24–25):4163–4172
- Shen X, Liu B, Li G et al (2014) Spatiotemporal change of diurnal temperature range and its relationship with sunshine duration and precipitation in China. *J Geophys Res Atmos* 119:13163–13179
- Sun XB, Ren GY, Bhaka SA et al (2017a) Changes in extreme temperature events over the Hindu Kush Himalaya during 1961–2015. *Adv Climate Change Res* 8(3):157–165
- Sun XB, Ren GY, Xu WH et al (2017b) Global land-surface air temperature change based on the new CMA GLSAT data set. *Sci Bull* 62(4):236–238
- Sun XB, Ren GY, You QL et al (2019) Global diurnal temperature range (DTR) changes since 1901. *Clim Dyn* 52(5):3343–3356
- Tang GL, Ding YH, Wang SW et al (2009) Comparative analysis of the time series of surface air temperature over China for the last 100 years. *Adv Climate Change Res* 2009 5(2):71–78 (in Chinese)
- Thorne PW, Parker DE, Christy JR et al (2005) Uncertainties in climate trends: lessons from upper-air temperature records. *Bull Am Meteorol Soc* 86(10):1437–1442
- Thorne PW, Menne MJ, Williams CN et al (2016) Reassessing changes in diurnal temperature range: a new data set and characterization of data biases. *J Geophys Res Atmos* 121(10):5115–5137
- Trenberth KE, Shea DJ (2005) Relationships between precipitation and surface temperature. *Geophys Res Lett* 32:L14703
- Varquez ACG, Kanda M (2018) Global urban climatology: a meta-analysis of air temperature trends (1960–2009). *Nature Partner J Climate Atmos Sci* 1:32. <https://doi.org/10.1038/s41612-018-0042-8>
- Vasseur DA, Delong JP, Gilbert B et al (2014) Increased temperature variation poses a greater risk to species than climate warming. *Proc Royal Soc B Biol Sci* 281(1779):20132612
- Vose RS, Easterling DR, Gleason B (2005) Maximum and minimum temperature trends for the globe: an update through 2004. *Geophys Res Lett* 32:L23822
- Wang J, Yan ZW, Feng JM (2018) Exaggerated effect of urbanization in the diurnal temperature range via “observation minus reanalysis” and the physical causes. *J Geophys Res Atmos* 123:7223–7237
- Wang K, Ye H, Chen F et al (2012) Urbanization effect on the diurnal temperature range: different roles under solar dimming and brightening. *J Clim* 25(3):1022–1027
- Wang KC, Dickinson RE (2013) Contribution of solar radiation to decadal temperature variability over land. *Proc Natl Acad Sci U S A* 110(37):14877–14882
- Wang KC, Dickinson RE, Liang SL (2009) Clear sky visibility has decreased over land globally from 1973 to 2007. *Science* 323(5920):1468–1470
- Wild M (2012) Enlightening global dimming and brightening. *Bull Am Meteorol Soc* 93(1):27–37
- Xu WH, Li QX, Jones PD et al (2017) A new integrated and homogenized global monthly land surface air temperature dataset for the period since 1900. *Clim Dyn* 15:1–24. <https://doi.org/10.1007/s00382-017-3755-1>
- Yang P, Ren GY, Liu W (2013) Spatial and temporal characteristics of Beijing urban heat island intensity. *J Appl Meteorol Climatol* 52(8):1803–1816
- Yang S, Xu W, Xu Y et al (2016) Development of a global historic monthly mean precipitation dataset. *J Meteorol Res* 30(2):217–231
- You QL, Min JZ, Jiao Y et al (2016) Observed trend of diurnal temperature range in the Tibetan plateau in recent decades. *Int J Climatol* 36(6):2633–2643
- Zhai PM, Pan XH (2003) Trends in temperature extremes during 1951–1999 in China. *Geophys Res Lett* 30(17):169–172

- Zhang AY, Ren GY, Zhou JX et al (2010) On the urbanization effect on surface air temperature trends over China. *Acta Meteorologica Sinica* 68(6):957–966 (in Chinese)
- Zhang PF, Ren GY, Qin Y et al (2021) Urbanization effects on estimates of global trends in mean and extreme air temperature. *J Climate* 34(5):1923–1945
- Zhao TB (2014) Correlation between atmospheric water vapor and diurnal temperature range over China. *Atmos Oceanic Sci Lett* 7(4):369–375
- Zhou LM, Dai AG, Dai YJ et al (2009) Spatial dependence of diurnal temperature range trends on precipitation from 1950 to 2004. *Clim Dyn* 32(2/3):429–440

Publisher's note Springer Nature remains neutral with regard to jurisdictional claims in published maps and institutional affiliations.

Affiliations

Xiubao Sun^{1,2,3} • **Chunzai Wang**^{1,2,3} • **Guoyu Ren**^{4,5}

¹ State Key Laboratory of Tropical Oceanography, South China Sea Institute of Oceanology, Chinese Academy of Sciences, Guangzhou 510301, China

² Southern Marine Science and Engineering Guangdong Laboratory (Guangzhou), Guangzhou 511458, China

³ Innovation Academy of South China Sea Ecology and Environmental Engineering, Chinese Academy of Sciences, Guangzhou 510000, China

⁴ Department of Atmospheric Science, School of Environmental Studies, China University of Geosciences, Wuhan 430074, China

⁵ Laboratory for Climate Studies, National Climate Center, China Meteorological Administration, Beijing 100081, China

Terms and Conditions

Springer Nature journal content, brought to you courtesy of Springer Nature Customer Service Center GmbH (“Springer Nature”).

Springer Nature supports a reasonable amount of sharing of research papers by authors, subscribers and authorised users (“Users”), for small-scale personal, non-commercial use provided that all copyright, trade and service marks and other proprietary notices are maintained. By accessing, sharing, receiving or otherwise using the Springer Nature journal content you agree to these terms of use (“Terms”). For these purposes, Springer Nature considers academic use (by researchers and students) to be non-commercial.

These Terms are supplementary and will apply in addition to any applicable website terms and conditions, a relevant site licence or a personal subscription. These Terms will prevail over any conflict or ambiguity with regards to the relevant terms, a site licence or a personal subscription (to the extent of the conflict or ambiguity only). For Creative Commons-licensed articles, the terms of the Creative Commons license used will apply.

We collect and use personal data to provide access to the Springer Nature journal content. We may also use these personal data internally within ResearchGate and Springer Nature and as agreed share it, in an anonymised way, for purposes of tracking, analysis and reporting. We will not otherwise disclose your personal data outside the ResearchGate or the Springer Nature group of companies unless we have your permission as detailed in the Privacy Policy.

While Users may use the Springer Nature journal content for small scale, personal non-commercial use, it is important to note that Users may not:

1. use such content for the purpose of providing other users with access on a regular or large scale basis or as a means to circumvent access control;
2. use such content where to do so would be considered a criminal or statutory offence in any jurisdiction, or gives rise to civil liability, or is otherwise unlawful;
3. falsely or misleadingly imply or suggest endorsement, approval, sponsorship, or association unless explicitly agreed to by Springer Nature in writing;
4. use bots or other automated methods to access the content or redirect messages
5. override any security feature or exclusionary protocol; or
6. share the content in order to create substitute for Springer Nature products or services or a systematic database of Springer Nature journal content.

In line with the restriction against commercial use, Springer Nature does not permit the creation of a product or service that creates revenue, royalties, rent or income from our content or its inclusion as part of a paid for service or for other commercial gain. Springer Nature journal content cannot be used for inter-library loans and librarians may not upload Springer Nature journal content on a large scale into their, or any other, institutional repository.

These terms of use are reviewed regularly and may be amended at any time. Springer Nature is not obligated to publish any information or content on this website and may remove it or features or functionality at our sole discretion, at any time with or without notice. Springer Nature may revoke this licence to you at any time and remove access to any copies of the Springer Nature journal content which have been saved.

To the fullest extent permitted by law, Springer Nature makes no warranties, representations or guarantees to Users, either express or implied with respect to the Springer nature journal content and all parties disclaim and waive any implied warranties or warranties imposed by law, including merchantability or fitness for any particular purpose.

Please note that these rights do not automatically extend to content, data or other material published by Springer Nature that may be licensed from third parties.

If you would like to use or distribute our Springer Nature journal content to a wider audience or on a regular basis or in any other manner not expressly permitted by these Terms, please contact Springer Nature at

onlineservice@springernature.com